J Fluoresc (2014) 24:875–884
DOI 10.1007/s10895-014-1365-4

ORIGINAL PAPER

Photoinduced Electron Transfer Reactions of Ruthenium(II)-Complexes Containing Amino Acid with Quinones

Rajkumar Eswaran · Swarnalatha Kalayar · Muthu Mareeswaran Paulpandian · Rajagopal Seenivasan

Received: 3 October 2013 / Accepted: 5 February 2014 / Published online: 4 March 2014

Abstract With the aim of mimicking, at basic level the photoinduced electron transfer process in the reaction center of photosystem II, ruthenium(II)-polypyridyl complexes, carrying amino acids were synthesized and studied their photoinduced electron transfer reactions with quinones by steady state and time resolved measurements. The reaction of quinones with excited state of ruthenium(II)-complexes, **I–V** in acetonitrile has been studied by luminescence quenching technique and the rate constant, k_q, values are close to the diffusion controlled rate. The detection of the semiquinone anion radical in this system using time-resolved transient absorption spectroscopy confirms the electron transfer nature of the reaction. The semiclassical theory of electron transfer has been successfully applied to the photoluminescence quenching of Ru(II)-complexes with quinones.

Keywords Ru(II) complex · Electron transfer · Quinone · Transient absorption

Introduction

Ruthenium(II)-polypyridyl complexes, $[Ru(NN)_3]^{2+}$ are having unique and advantageous photophysical properties [1, 2]. The application of $[Ru(NN)_3]^{2+}$ complexes are varied from solar energy conversion [3–5] as photocatalysts [6–8] sensors for biomolecules [9–11] to phototherapeutic agents [12, 13]. The excited state properties of these complexes can be varied systematically by changing the structure of the ligands [1, 14, 15]. For instance several amide moiety incorporated polypyridyl ligands have been synthesized to mimic the function of peptides and proteins and these were used for the synthesis of ruthenium(II)-polypyridyl complexes [16–19]. Metal containing amino acids and peptides are key components for the study of photoinduced energy and electron transfer processes [15–29]. These organic–inorganic hybrid molecules have been assembled via different routes: (i) metal complexes coordinate to the donor-containing natural amino acids (e.g.histidine) [21] (ii) attachment of metal complexes to peptide termini [24, 25] (iii) synthesis of chelator ligands which contain amino acids followed by metal coordination [20, 26–29].

In Photosystem, quinones are ultimate electron acceptors, on excitation of primary electron donor chlorophyll, P_{680}, with a light quantum, an electron is transferred to the primary electron acceptor, phenophytin and subsequently to the quinones Q_A and Q_B [30–33]. Quinones are appear to be predestined as electron acceptors in nature for a variety of reasons and some key factors are (i) quinones possess favorable redox potentials, (ii) they can be converted stepwise into stable reduction products such as hydroquinones via

Electronic supplementary material The online version of this article (doi:10.1007/s10895-014-1365-4) contains supplementary material, which is available to authorized users.

R. Eswaran · S. Kalayar · M. M. Paulpandian · R. Seenivasan (✉)
School of Chemistry, Madurai Kamaraj University,
Madurai 625 021, India
e-mail: rajagopalseenivasan@yahoo.com

R. Eswaran (✉)
Department of Chemistry, Vel Tech University, Avadi, Chennai, India
e-mail: rajjkumar_e@yahoo.com

S. Kalayar
Department of Chemistry, Manonmaniam Sundaranar University,
Thirunelveli, India

M. M. Paulpandian
Department of Chemical and Biomolecular Engineering, Korea
Advanced Institute of Science and Technology,
Daejeon, South Korea

semiquinones, (iii) they are capable of forming hydrogen bonds and (iv) they are relatively small molecules with a high mobility and, as a result, can shuttle redox equivalents to the quinone pool [34]. In order to understand the electron accepting properties of quinones in natural photosynthesis, several model photosensitizers (metal-porphyrin, ruthenium(II)-polypyridyl complexes) have been designed and ET reactions with quinones, inter- and intramolecular have been studied [20, 35–39]. In these reactions the formation of semiquinone anion radical as the transient has been established using time resolved techniques [40]. In order to mimic the important light driven process in photosystem II, many efforts have been made in recent years where Ru(II)-polypyridine complexes were used as model photosensitizers and quinones as electron acceptors. Herein, we report a detailed study on the excited state electron transfer reactions of Ru(II)-polypyridyl complexes carrying amino acids with quinones using steady state and flash photolysis measurements. The formation of quinone anion radical has been studied using the transient absorption techniques. Semiclassical theory of electron transfer is applied successfully for the photoluminescence quenching of ruthenium(II)-complexes with quinones.

Experimental Section

Materials and Methods

The ligand 2,2′-bipyridine (bpy), quinones and $RuCl_3.3H_2O$ were obtained from Merck and Aldrich and used as such. The ligands and ruthenium(II)-complexes **I–V** were synthesized by known reported procedures [20, 38]. The details of experimental methods were given in the Supporting information.

Determination of Bimolecular Luminescence Quenching Rate Constants

The luminescence quenching of excited state Ru(II) complexes **I–V** with quinones has been studied by luminescence intensity quenching technique. The luminescence measurements were performed at different quencher concentration and the quenching rate constant, k_q, values were determined from the Stern-Volmer plot using the equation given below [2].

$$I_0/I = 1 + K_{sv}[Q] = 1 + k_q\tau_0[Q] \quad (1)$$

Where I_0 and I are the luminescence intensities of Ru(II) complexes in the absence and presence of quencher respectively, K_{sv}, the Stern-Volmer constant, [Q] is the concentration of quencher, τ_0 the luminescence lifetime of the Ru(II) complexes in the absence of quencher and k_q, is the bimolecular quenching rate constant.

Results and Discussion

Photophysical Properties of Ruthenium(II)-Complexes

The structure of the ruthenium(II)-complexes (**I–V**) used in the present study were shown in Chart 1. The electronic absorption and emission spectroscopic data, excited state lifetime and excited state redox potential data for ruthenium(II)-complexes (**I–V**) measured in acetonitrile are listed in Table 1. The absorption and emission spectra of all five complexes (**I–V**) exhibit the characteristic bands found in the parent ruthenium(II) complex, $[Ru(bpy)_3]^{2+}$ and its derivatives [35, 36]. The intense absorption band at ~288 nm is assigned to ligand centered transitions (π-π*) and the band in the visible region (455–458 nm) to the metal-to-ligand charge transfer (MLCT) transition (dπ(Ru) → π*(ligand)). The absorption and emission spectra of ruthenium(II) complex, **V**, $[Ru(bpy)_2$(4-Me-4′-(CONH-L-phenylalanine ethyl ester)-2,2′-bpy)$](PF_6)_2$ in CH_3CN is shown in Fig. 1. The ruthenium(II) complexes **I–V** exhibit intense and long lived luminescence in acetonitrile solution at 298 K. The emission maxima of complexes **I–V** occur at 621–644 nm in acetonitrile at 298 K (Table 1). It has been well established that, the excited state properties like emission energy and lifetime of the ruthenium(II)-polypyridine complexes can be finely tuned by introduction of different functionalities onto the ligand systems and medium [20, 41, 42]. The emission energy of the Ru(II) complexes used in the present study is slightly lower than that of parent complex, $[Ru(bpy)_3]^{2+}$ and this can be attributed to the acceptor character of the ligand orbital. This in turn is due to the presence of the low lying π* orbital of the carboxylic acid and amide containing diimine ligands owing to the electron withdrawing nature of $–CO_2H$ and amide functionality [18–20, 41, 42]. Though λ_{max} of MLCT absorption of all complexes is red shifted only to the tune of 6–8 nm compared to that of parent complex, $[Ru(bpy)_3]^{2+}$, the emission maximum is red shifted to the tune of 16–24 nm when the amino acid moiety is introduced in the bpy ligand.

Reactions of Excited State I–V with Quinones

The structures of the quenchers used in the present study are shown in Chart 2. The reactions of excited state **I–V** with quinones have been studied by luminescence quenching technique and the observed quenching rate constant, k_q, data are collected in Table 2. The k_q data given in Table 2 show that the value of k_q is sensitive to the reduction potential of quinones. Quinones form ground state complexes with $[Ru(NN)_3]^{2+}$ due to charge transfer and π-π stacking interactions which is supported by spectroscopic changes and positive shift in the reduction potential of quinones. In order to check the ground state complex formation between Ru(II) complexes **I–V** and quinones we recorded the absorption spectrum of a mixture of

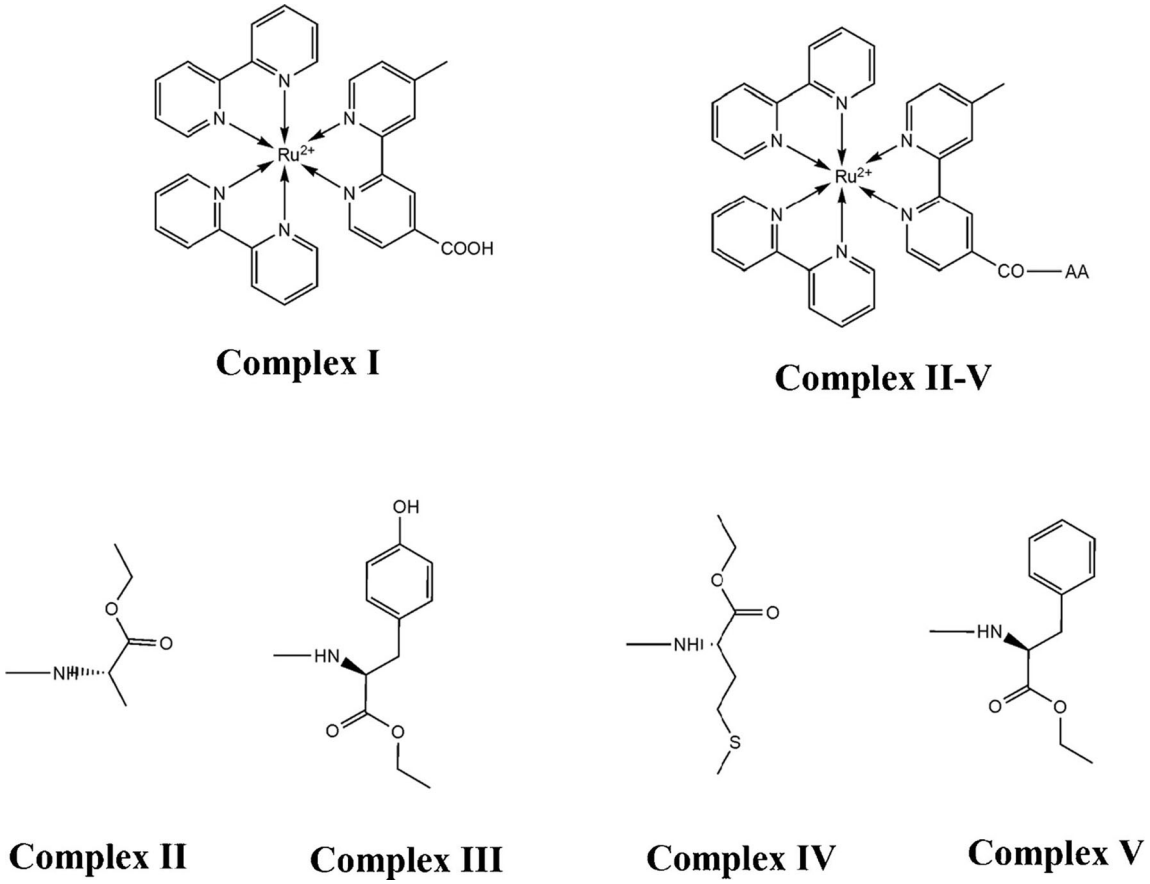

Chart 1 Structure of ruthenium(II)-complexes

a Ru(II) complex and quinone using concentrations of reactants similar to those used in the quenching studies. The absorption spectra of these mixtures were shown to be equal to those expected by adding the spectra from separate solutions of donor and quencher. No evidence was obtained for the formation of the ground state complex between Ru(II) complexes, **I–V** and quinones, under the experimental conditions used, based on absorption spectroscopic studies (Figures S1–S2). From the redox potential data shown in Table 1, the values of free energy change ΔG^0, for the photoinduced electron transfer between the excited state of **I–V** and quinones have been calculated (vide infra). It is apparent from the data in Table 2 that quinones with higher reduction potentials exhibit higher quenching rate constants, a trend that is indicative of electron transfer quenching.

Stern-Volmer Analysis

The emission intensities (I) of complexes **I–V**, are efficiently quenched in the presence of quinones in acetonitrile and are analyzed in terms of the Stern-Volmer relationship (Eq. 1). Figure 2 shows that the change of emission intensity of complex, **V** with different [DCBQ]. A typical Stern-Volmer

Table 1 Absorption maxima, λ_{abs}^{max}, nm, emission maxima, λ_{em}^{max}, nm, excited state lifetime (in ns) and the redox potential values of Ru(II)-polypyridyl complexes **I–V** in acetonitrile at 298 K

Complex	Absorption maxima, nm	Emission maxima, nm	Excited state lifetime, ns	E^0_{oxd}, V	$E^{*3+/2+}_{Ru}$, V
$[Ru(bpy)_3]^{2+}$	450,423,288	620	850	+1.26	−0.84
$[Ru(bpy)_2(cmbpy)]$, **I**	455,288,246	621	995	+1.36	−0.74
$[Ru(bpy)_2(mbpy\text{-}ala)]$, **II**	456,287,245	636	1,224	+1.37	−0.73
$[Ru(bpy)_2(mbpy\text{-}tyr)]$, **III**	458, 288,246	644	1,250	+1.32	−0.78
$[Ru(bpy)_2(mbpy\text{-}met)]$, **IV**	457,287,246	636	721	+1.39	−0.71
$[Ru(bpy)_2(mbpy\text{-}phe)]$, **V**	458,288,247	640	1,280	+1.35	−0.75

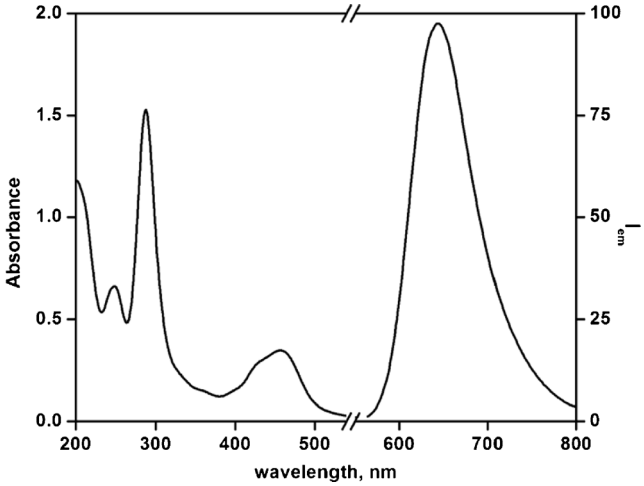

Fig. 1 Absorption and emission spectra of complex **V**, [Ru(bpy)$_2$(4-Me-4′-(CONH-L-phenylalanine ethyl ester)- 2,2′-bpy)] in acetonitrile at RT

plot for the oxidative quenching of **IV** with quinones obtained from luminescence intensity measurements is given in the Fig. 3. The linearity of the Stern-Volmer plot indicates that there is no ground state complex formation between Ru(II) complex and the quencher (*vide infra*). The emission decay times of ruthenium(II)-complexes decreases with increasing concentration of the quenchers. No deviation from the single exponential decay could be detected even at the larger concentrations of the quenchers employed. The χ^2 of the fitting were always in the range of 1.01–1.20, while applying bi-exponential or multi-exponential decay models to the analysis of the emission decays do not lead to significant improvements of χ^2 or residuals plots. Figure 4 represents the lifetime quenching of complexes **IV** and **V** with different concentrations of 2,6-dichlorobenzoquinone.

The linear Stern-Volmer plots and the k_q values obtained from luminescence measurements suggest that the quenching

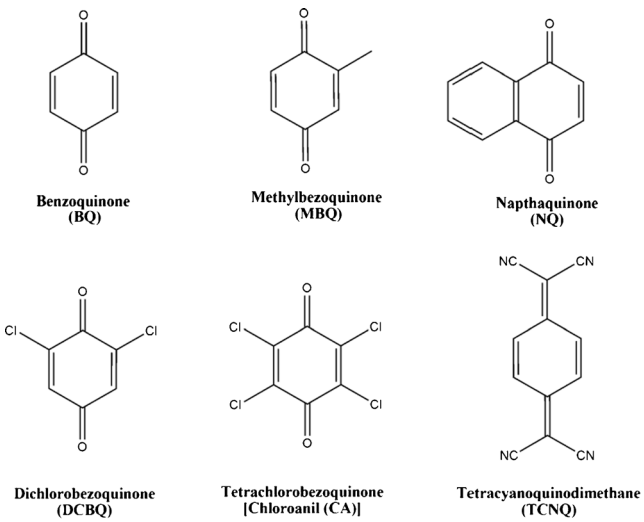

Chart 2 Structure of quinone used in the present study

of complexes **I–V**, with quinones is dynamic in nature and the quenching process can be explained using Scheme 1. According to Scheme 1, the excited state donor ($*Ru^{II}$) and the ground state acceptor (quinone) molecules diffuse together to form an encounter complex, ($*Ru^{II\cdots}Q$). This encounter complex then undergoes a reorganization to reach the transition state where ET takes place from the donor to the acceptor to give an ion-pair species, ($Ru^{III\cdots}Q^{-}$), the successor complex. The parameters k_{12} and k_{21} are the diffusion-controlled rate constants for the formation and dissociation of the encounter complex ($*Ru^{II}\cdots Q$), respectively. The k_{23} and k_{32} are the forward and reverse ET rate constants. Apart from the back electron transfer to form the precursor complex (k_{32}) the ion-pair state, ($Ru^{III}\cdots Q^{-\cdot}$), can form the separated species $Ru^{III}\cdots Q^{-}$ (k_{sep}) and undergo back electron transfer to form the reactants in the ground state (k_{34}).

In order to treat the dynamic quenching process in terms of thermodynamic function (ΔG^0), we correlated the electron transfer rate constant, k_{23}, values estimated from the k_q values with the free energy change (ΔG^0) of the electron transfer process (cf. Eq. 3 for details of calculating k_{23} from k_q). The plot of log k_{23} vs ΔG^0 is shown in Fig. 5 and the electron transfer rate constant increases with increasing the driving force (ΔG^0) of the electron transfer reaction and attains saturation at high $-\Delta G^o$ values.

Transient Absorption Spectra

To confirm the electron transfer nature of the reaction from the excited state Ru(II) complexes **I–V** to quinone, transient absorption spectrum of the reaction mixture has been recorded using flash photolysis technique. Argon bubbled acetonitrile solutions of Ru(II) complexes were excited at 355 nm under laser flash photolysis. The transient difference absorption spectra of complex **V** in CH_3CN at various time delays are shown in supporting information (Figure S3). The spectrum, at each time delay, consists of bleach around 450 nm due to the loss of ground state absorption, dπ-π* (MLCT) transition and a positive absorption with maxima centered at 370 and

Table 2 Bimolecular quenching rate constants, k_q, for the oxidative quenching of $*[Ru(NN)_3]^{2+}$ complexes by quinones in CH_3CN at 298 K

Quencher	k_q, M^{-1} s^{-1}				
	I	II	III	IV	V
TCNQ	2.0×10^{10}	1.5×10^{10}	1.0×10^{10}	2.1×10^{10}	2.0×10^{10}
CA	1.1×10^{10}	8.6×10^{9}	9.0×10^{9}	1.7×10^{10}	1.5×10^{10}
DCBQ	1.0×10^{10}	8.2×10^{9}	9.1×10^{9}	1.3×10^{10}	9.9×10^{9}
BQ	6.2×10^{9}	7.9×10^{9}	8.0×10^{9}	9.9×10^{9}	1.4×10^{9}
MBQ	1.6×10^{9}	2.4×10^{9}	4.3×10^{9}	3.1×10^{9}	2.0×10^{9}
NQ	4.1×10^{9}	3.8×10^{9}	4.4×10^{9}	4.1×10^{9}	4.9×10^{9}

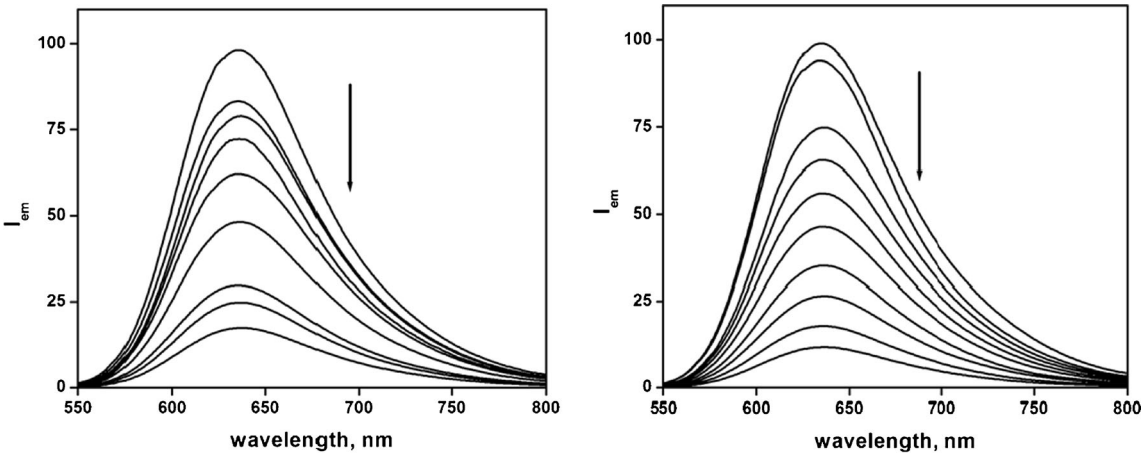

Fig. 2 Change of luminescence intensity of **IV** with different [quinone]. **a** benzoquinone (2×10^{-5}–6×10^{-4} M) **b** TCNQ (2×10^{-5}–2×10^{-4} M)

555 nm corresponding to the formation of substituted bipyridyl anion radical (L^{-}) [17–20, 43–45]. Quenching and the progress of the reaction of the long-lived excited state of $[Ru(NN)_3]^{2+}$ with tetrachlorobenzoquinone (chloranil, CA) was followed using time-resolved absorption studies by means of <8 ns laser width at 355 nm excitation. Figures 6 and 7 show the transient absorption spectra of **II** and **IV** recorded in the absence and presence of 100 μM chloranil obtained after 2 μs following laser flash as a function of wavelength.

In Figures 6 and 7, in the presence of chloranil, a new transient species is formed around 440 nm. The broad band around 440 nm was assigned to the quinone anion radical [46–50]. The absorption at 440 nm is caused by the formation of quinone anion radical upon oxidation of *Ru(II) with quinone, while there is no positive signal in this region when we have the complexes **II** and **IV** alone. Giacco et al. [48] investigated the photochemical behavior of alkyl aryl sulfides sensitized by triplet chloranil by nanosecond laser flash photolysis and steady state irradiation in organic solvents. Similarly complex **VI** undergo electron transfer reaction with DCBQ. The dynamics of transient, quinone anion radical formed at 410 nm from the redox system complex, **IV** (80 μM) and DCBQ, (300 μM) was followed and the kinetic traces observed in the absence and presence of DCBQ are shown in Fig. 8.

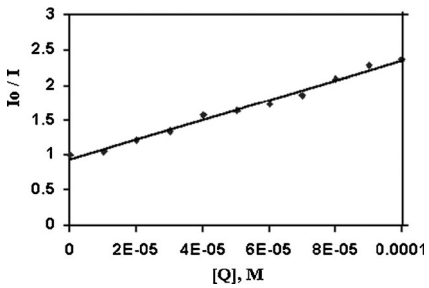

Fig. 3 Stern-Volmer plot for the oxidative quenching of complex **IV** with [TCNQ]

This supports the formation of quinone anion radical (absorption at 410 nm) due to the ET from *Ru(II) complex to the quinone. The decay of the long lived quinone anion radical is shown in Figure S4 and the radical has half lifetime in the range of ~19 μs [50]. The quinone anion radicals are usually long lived and they have lifetime in the range of few μs to seconds depending on the experimental conditions.

Dynamics of Electron Transfer Reactions of Ru(II) Complexes with Quinones

The rate of ET from a donor molecule to an acceptor in a solvent is controlled by free energy change of the reaction (ΔG^0), the reorganization energy (λ) and the electron transfer distance (d) between the donor and the acceptor. The ET rate constant (k_{et}) in both the classical and semiclassical theories can be represented by Eq. (2) [51–54].

$$k_{et} = \kappa_{el}\upsilon_n \exp\left[-\Delta G^{\#}/(RT)\right] \quad (2)$$

where κ_{el} is the electronic transmission coefficient, υ_n the nuclear frequency and $\Delta G^{\#}$ is the free energy of activation. When the electron transfer distance, d, is kept constant, the rate of the ET process is decided by ΔG^0 and the reorganization energy, λ, through the Marcus equation (Eq. 3) [51–54].

$$\Delta G^{\#} = \left(\lambda + \Delta G^0\right)^2/(4\lambda) \quad (3)$$

Substitution of the above expression into Eq. (4) gives the basic relation for k_{et} in terms of ΔG^0 and λ:

$$k_{et} = \kappa_{el}\upsilon_n \exp\left[-\left(\lambda + \Delta G^0\right)^2/(4\lambda RT)\right] \quad (4)$$

The value of $\kappa_{el}\,\upsilon_n$ is usually taken as 1.0×10^{11} s^{-1}.

According to classical Marcus theory ET can occur only at the intersection point of the two potential energy surfaces. In such case, a more effective route for the electron transfer rate

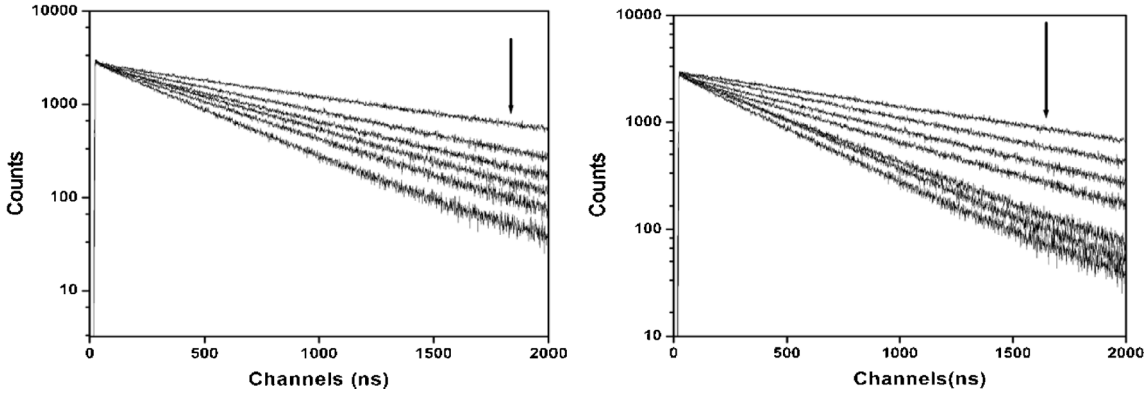

Fig. 4 Life time quenching of complexes **IV** and **V** with different [DCBQ]. (1×10^{-4}–5×10^{-4} M)

is derived from the semiclassical theory which can be represented by Eq. (5).

$$k_{et} = 4\pi^2/h|H_{DA}|^2(4\pi\lambda_O kT)^{-1/2}\sum_{m=0}^{\infty}\left(e^{-S}S^m/m!\right) \qquad (5)$$

$$\exp\left[-(\lambda_O + \Delta G^\circ + mh\nu)^2/4\lambda_O kT\right]$$

In Eq. (5) H_{DA} is the electronic coupling coefficient between the redox centers, the reorganization energy λ is composed of solvational λ_o and vibrational λ_i contributions with $s=\lambda_i/h\nu$, ν is the high-energy vibrational frequency associated with the acceptor and m is the density of product vibrational levels. The terms h and k are Planck's and Boltzmann's constants, respectively.

According to Rehm and Weller, the free-energy change of electron transfer ($\Delta G°$) can be calculated from Eq. 6 [53, 54].

$$\Delta G^\circ = E_{(D/D^+)} - E_{(A/A^-)} - E_{O-O} - e^2/a\varepsilon \qquad (6)$$

where $E(D/D^+)$ is the oxidation potential of donors, $E(A/A^-)$, the reduction potential of acceptor, E_{o-o} the lowest excited state energy of Ru(II) complexes, and $e^2/a\varepsilon$ a coulombic term. The $\Delta G°$ values thus estimated for different donor and acceptor pairs in CH_3CN are given in the Table 3.

The value of λ_o can be evaluated classically by using dielectric continuum model, Eq. 6.

$$\lambda_O = e^2/4\pi\varepsilon_O(1/2r_D + 1/2r_A - 1/d)\left(1/D_{op} - 1/D_S\right) \qquad (7)$$

where e is the transferred electronic charge, ε_o the permittivity of free space, D_{op} and D_s the optical and static dielectric constants, respectively. The terms r_D and r_A are the radii of the electron donor and acceptor, respectively and d is the separation distance between the donor and acceptor in the encounter complex. This model is most applicable in cases where the donor and acceptor are roughly spherical, and their center-to-center distance (r_{DA}) is large compared to the sum of the sphere radii. The values for r_D and r_A can be estimated by the MM2 molecular model (7.1 Å for **I**, 7.41 Å for **II** and 7.63 Å for **III**; 7.49 Å for **IV** and 7.61 Å for **V** and for quinones in the range 2.97 Å–5.0 Å). Since the ΔG^0 and λ values are known the value of rate constant for electron transfer from excited state ruthenium(II)-complexes to quinone can be calculated. In Eq. 4, $H_{DA}=2\times10^{-3}$ eV, λ=0.81–0.92 eV, ν=1,000–1,500 cm^{-1} and T=298 K. These values are the optimum values for the reaction, chosen by a trial and error method [55].

Since the quenching process occurs via ET, the redox quenching process can be discussed in terms of the mechanism shown in Scheme 1. By applying steady-state treatments to the short lived species in Scheme 1, the following expression (Eq. 8) for the observed bimolecular quenching rate constant, $k_{obs}(k_q)$ can be derived.

$$kq = \frac{k_{12}}{1 + \left(k_{12}/k_{23}K_{eq}\right)} \qquad (8)$$

K_{eq} is the equilibrium constant for the formation of the encounter complex and k_{12} is the rate constant for the

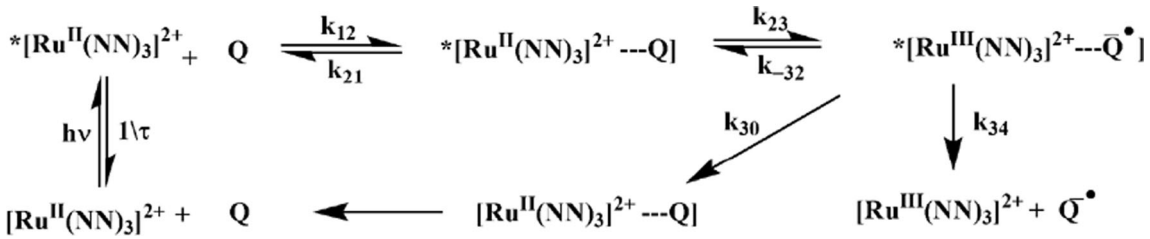

Scheme 1 Mechanism for the oxidative quenching of $[Ru(NN)_3]^{2+}$ with quinones

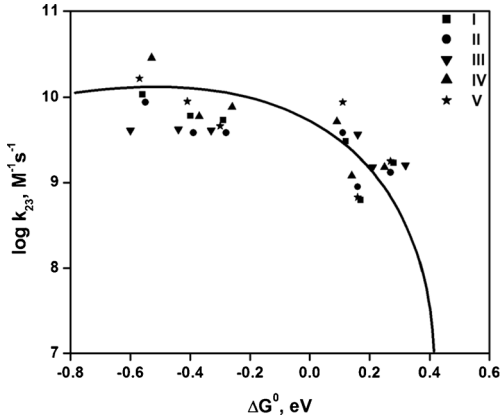

Fig. 5 Plot of log k_{23}, M^{-1} s^{-1} vs ΔG^0, eV for the oxidative quenching of **I–V** with quinones

diffusion process to form the encounter complex. The value of k_{12} is calculated from Eq. 9 [51–54].

$$k_{12} = 2RT/3000\eta[2 + r_D/r_A + r_A/r_D]f \quad (9)$$

where $f^{-1}=\mathrm{d}\int e^{u}/kT\,\mathrm{d}r/r^2$ with $u=Z_DZ_Ae^2/D_S[e^{Kd}/1+Kd]\,e^{-Kr}/r$ where $K=(8\pi e^2N\eta/1000D_SkT)^{1/2}$ and r_D and r_A are the radii of the reactants and η is the viscosity of the medium.

The diffusion rate constant, k_{12}, calculated according to Smoluchowski [56] for non-charged molecules, has a value of 1.9×10^{10} dm^3 mol^{-1} s^{-1}. K_{eq} was estimated using the Fuoss and Eigen equation (Eq. 10) [57].

$$K_{eq} = \left(4\pi Nd^3/3000\right)\exp(-w^r/RT) \quad (10)$$

where w^r is the work required to bring the reactants to the separation distance d. Since we use neutral quenchers throughout this study, w^r is zero. The value of K_{eq} is found to be in the range 2.56 to 8.03 M^{-1} for the oxidative quenching of ruthenium(II) complexes **I–V** with quinones. Since the values of k_{12} and K_{eq} are known the value for k_{23}, the rate constant for the process of ET in the encounter complex can be calculated from the observed k_q values using Eq. 8 and the values are plotted against ΔG^o in Fig. 5 for all five Ru(II)-complexes, **I–V**.

From the redox potential data shown in Tables 1 and 3, the values of free energy change ΔG^0, for the photoinduced electron transfer between the excited state of **I–V** and quinones have been calculated (*vide infra*). In order to treat the dynamic quenching process in terms of thermodynamic function (ΔG^0), we correlated the electron transfer rate constant, k_{23}, values estimated from the k_q values with the free energy change (ΔG^0) of the electron transfer process (cf. Eq. 8 for details of calculating k_{23} from k_q). The plot of log k_{23} vs ΔG^0 is shown in Fig. 5 and the electron transfer rate constant increases with increasing the driving force (ΔG^0) of the electron transfer reaction and attains saturation at high ΔG^o values (−0.2 eV). The values of k_{23} (k_{et}) can also be calculated using semiclassical theory from Eq. 4. The experimental k_{23} values along with the calculated k_{et} (solid line) values were plotted against $-\Delta G°$ values (Fig. 5) for all Ru(II) complexes.

The quenching rate constant k_q in Table 2 show that the variation in k_q with the change of $\Delta G°$ is by one order and most of the values are diffusion controlled rate. It is worthwhile to compare the results observed for the luminescence quenching of complexes **I–V** with quinones. In order to understand the effect of changing the structure of the ligand on the rate of the electron transfer it is necessary to maintain $\Delta G°$ values constant. Figure 5 shows that at a particular $\Delta G°$ (0.11 eV), the rate constant increases in the following order: **I** < **III** ~ **V**. Though complexes **III** and **V** contain bulky phenyl moiety in the ligand, the k_q values for complexes **III** and **V** are five times more than that of complex **I** at similar $\Delta G°$ value. The most probable explanation for this interesting observation is that the complex containing phenyl moiety in the bipyridine ligand is able to form π-π interaction with the quinones. Hoffmann et al. [58] have already established the importance of the π-π stacking between phenols and $[Ru(bpy)_3]^{2+}$. Figure 5 shows that the rate constants for ET reaction of chosen redox system are in accordance with Rhem- Weller model.

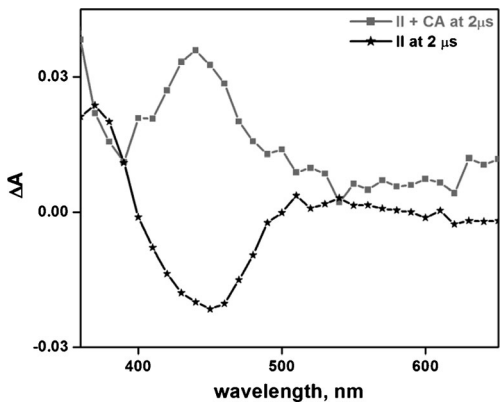

Fig. 6 Transient absorption spectrum of **II** in the presence of chloranil in acetonitrile at 298 K recorded 3 μs after laser flash

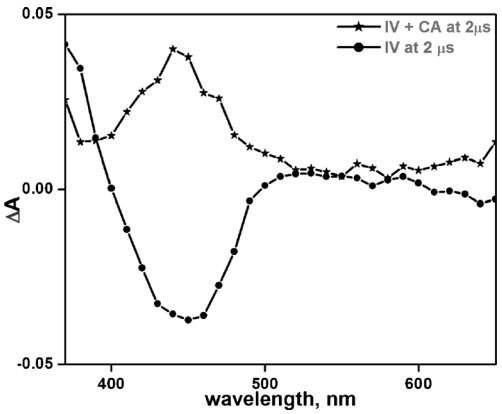

Fig. 7 Transient absorption spectrum of **IV** in the presence of chloranil in acetonitrile at 298 K recorded 3 μs after laser flash

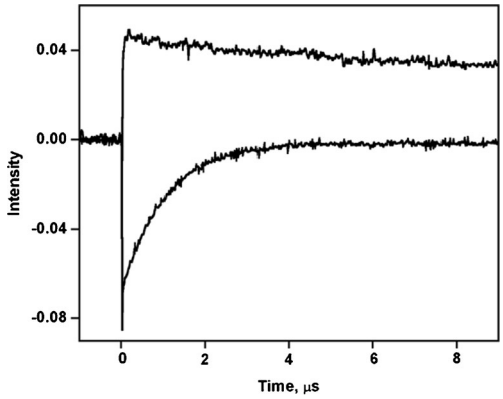

Fig. 8 The transient kinetics of complex **IV** (1×10^{-4} M) were measured at 410 nm in the absence and presence of DCBQ(1×10^{-3} M) (complex **IV**- lower traces; complex **IV** and DCBQ, upper traces)

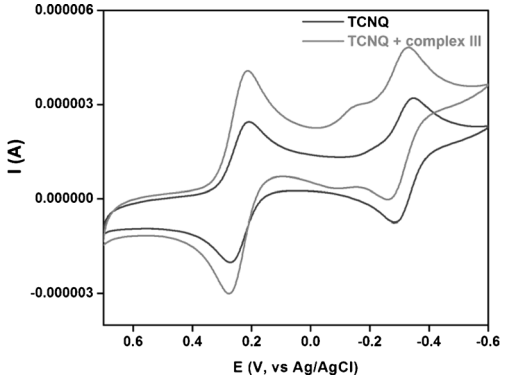

Fig. 9 Cyclic voltammogram of TCNQ in the absence and in the presence of complex **III**

CV Studies of $[Ru(NN)_3]^{2+}$ and Quinones

Cyclic voltammetric studies were performed in order to visualize the existence of any electronic interactions between the Ru(II)-complexes and quinones in the ground state. There is little change in the absorbance of MLCT band of $[Ru(NN)_3]^{2+}$ in the presence of different concentrations of quinone (Figures S1-S2). Three types of interactions may be attributed to the complex formation of quinones with electron donors: (i) charge transfer (EDA) interaction, (ii) hydrogen bond formation and (iii) π-π stacking. To get further experimental evidence for the interaction between electron donor and quinone we have recorded cyclic voltammograms (CV) of 2,6-dichlorobenzoquinone and TCNQ in the absence and presence of $[Ru(NN)_3]^{2+}$ complexes and the sample voltammogram is shown in Fig. 9.

The CV of 2,6-dichlorobenzoquinone shows two reduction waves one at −0.13 V and the other at −0.48 V. These reduction potentials can be attributed to DCBQ/$DCBQ^{-}$ and $DCBQ^{-}$/$DCBQ^{2-}$ couples. The addition of complexes **III** and **V** leads to an increase in the peak currents of DCBQ along with a slight shift in the peak potentials 50 mV for the first reduction and 90 mV for second reduction processes for complex **V** and 30 mV for the complex **III**. Cyclic voltammetry of TCNQ in a 0.1 M solution of $[NBu_4][ClO_4]$ in CH_3CN afforded two redox couples located at $E_{1/2}$=0.23 V and at $E_{1/2}$=−0.36 V vs Ag/AgCl. The addition of **III** (1.0×10^{-4} M) to TCNQ (1.0×10^{-4} M) increases the peak currents of TCNQ substantially accompanied by a shift in the peak potentials 60 and 10 mV in the first and the second reduction processes. The substantial increase in peak currents, accompanied by a slight shift in peak potentials constitutes valid experimental evidence in favor of the ground state interaction between complex **III** with quinone. Similar positive shift in the reduction potential of quinone has been observed in several cases where host-guest interaction is possible [59–61]. In the present study, we attribute the interaction to charge transfer as well as π-π interaction between the aromatic rings of the ligand and the aromatic rings of quinones. The π-π stacking has also been proposed between phenols and $[Ru(bpy)_3]^{2+}$ [58]. The cyclic voltammetric studies provide support for weak ground state interaction between the Ru(II) complex and the quencher, quinone. Thus the weak π-π interaction in the ground state is responsible for higher k_q values observed for complexes **III** and **V** compared to complexes **I**. If the ground state interaction is strong we have to consider the importance of static quenching also in the overall quenching process. As the ground state interaction between Ru(II) complexes and quinones used in this system is weak we did not make any attempt to resolve the total k_q values into static and dynamic quenching contributions.

Table 3 ΔG^0 (eV), values for the quenching of $*[Ru(NN)_3]^{2+}$ with quinones in acetonitrile at 298 K

Quencher	E^0_{red}, V	ΔG^0, eV				
		I	II	III	IV	V
TCNQ	−0.18	−0.56	−0.55	−0.60	−0.53	−0.57
CA	−0.34	−0.40	−0.39	−0.44	−0.37	−0.41
DCBQ	−0.45	−0.29	−0.28	−0.33	−0.26	−0.30
BQ	−0.86	0.12	0.11	0.16	−0.09	0.11
MBQ	−0.91	0.17	0.16	0.21	0.14	0.16
NQ	−1.02	0.28	0.27	0.32	0.25	0.27

Conclusion

The photoinduced electron transfer reactions of ruthenium(II)-complexes (**I–V**) with quinones were studied by luminescence and laser flash photolysis method. From the transient absorption spectra and luminescence quenching data clearly show that the excited state of ruthenium(II) complexes (**I–V**) undergo rapid ET reactions with quinones. The observation of quinone anion radical supports the ET quenching of ^{3}MLCT

excited state of ruthenium(II) complexes with quinone. The quenching rate constant, k_q, is close to the diffusion limited rate at high negative $\Delta G°$ values and the k_q values are well correlated with the $\Delta G°$ values. In addition, semiclassical theory of ET was successfully applied to the photoluminescence quenching process.

Acknowledgments S.R thanks DST, New Delhi for sanctioning a project. E.R thanks to CSIR, New Delhi, India for the award of Senior Research Fellowship. The authors thank Prof. P. Ramamurthy, NCUFP, University of Madras and NCFRR, University of Pune for flash photolysis and TCSPC measurements.

References

1. Kalyanasundaram K (1992) Photochemistry of polypyridine and porphyrin complexes. Academic, London
2. (2006) Quenching of fluorescence. In: Lakowicz J (ed) Principles of fluorescence spectroscopy. Springer US, pp 277–330
3. Gratzel M (2001) Photoelectrochemical cells. Nature 414:338–344
4. Grätzel M (2005) Solar energy conversion by dye-sensitized photovoltaic cells. Inorg Chem 44:6841–6851
5. Giribabu L, Singh VK, Vijay Kumar C, Soujanya Y, Gopal Reddy V, Yella Reddy P (2011) Organic-ruthenium(II) polypyridyl complex based sensitizer for dye-sensitized solar cell applications. Adv OptoElectron 2011:8
6. Lele Duan FB, Mandal S, Stewart B, Privalov T, Llobet A, Sun L (2012) A molecular ruthenium catalyst with water-oxidation activity comparable to that of photosystem II. Nat Chem 4:418–423
7. Chen Z, Chen C, Weinberg DR, Kang P, Concepcion JP, Harrison DP, Brookhart MS, Meyer TJ (2011) Electrocatalytic reduction of CO_2 to CO by polypyridyl ruthenium complexes. Chem Commun 47: 12607–12609
8. Ohzu S, Ishizuka T, Hirai Y, Fukuzumi S, Kojima T (2013) Photocatalytic oxidation of organic compounds in water by using ruthenium(II)–pyridylamine complexes as catalysts with high efficiency and selectivity. Chem Eur J 19:1563–1567
9. Muthu Mareeswaran P, Babu E, Rajagopal S (2013) Optical recognition of anions by ruthenium(II)-bipyridine-calix[4]arene system. J Fluoresc 23:997–1006
10. Babu E, Muthu Mareeswaran P, Rajagopal S (2013) Highly sensitive optical biosensor for thrombin based on structure switching aptamer-luminescent silica nanoparticles. J Fluoresc 23:137–146
11. Muthu Mareeswaran P, Maheshwaran D, Babu E, Rajagopal S (2012) Binding and fluorescence resonance energy transfer (FRET) of ruthenium(II)-bipyridine-calixarene system with proteins—experimental and docking studies. J Fluoresc 22:1345–1356
12. Taheri S, Behzad M, Nazari H, Khaleghian A (2013) Synthesis, characterization, and biological studies of new ruthenium polypyridyl complexes containing noninnocent ligands. ISRN Inorg Chem 2013:6
13. Gill MR, Thomas JA (2012) Ruthenium(ii) polypyridyl complexes and DNA-from structural probes to cellular imaging and therapeutics. Chem Soc Rev 41:3179–3192
14. Szaciłowski K, Macyk W, Drzewiecka-Matuszek A, Brindell M, Stochel G (2005) Bioinorganic photochemistry: frontiers and mechanisms. Chem Rev 105:2647–2694
15. Batista ER, Martin RL (2005) On the excited states involved in the luminescent probe $[Ru(bpy)_2dppz]^{2+}$. J Phys Chem A 109:3128–3133
16. Barton J (1986) Metals and DNA: molecular left-handed complements. Science 233:727–734
17. Mecklenburg SL, Peek BM, Schoonover JR, McCafferty DG, Wall CG, Erickson BW, Meyer TJ (1993) Photoinduced electron transfer in amino acid assemblies. J Am Chem Soc 115:5479–5495
18. McCafferty DG, Bishop BM, Wall CG, Hughes SG, Mecklenberg SL, Meyer TJ, Erickson BW (1995) Synthesis of redox derivatives of lysine and their use in solid-phase synthesis of a light-harvesting peptide. Tetrahedron 51:1093–1106
19. Hurley D, Roppe JR, Tor Y (1999) Coordination compounds as building blocks: simple synthesis of RuII-containing amino acids and peptides. Chem Commun 993–994
20. Rajkumar E, Rajagopal S, Ramamurthy P, Vairamani M (2009) Photophysics of ruthenium(II) complexes carrying amino acids in the ligand 2,2′-bipyridine and intramolecular electron transfer from methionine to photogenerated Ru(III). Inorg Chim Acta 362:1629–1636
21. Chang IJ, Gray HB, Winkler JR (1991) High-driving-force electron transfer in metalloproteins: intramolecular oxidation of ferrocytochrome c by $[Ru(2,2′\text{-bpy})_2(im)(his\text{-}33)]^{3+}$. J Am Chem Soc 113:7056–7057
22. Geißer B, Alsfasser R (2003) A peptide approach to covalently linked $[Ru(bipy)_3]^{2+}$–ferrocene and $[Ru(bipy)_3]^{2+}$–tyrosine conjugates. Inorg Chim Acta 344:102–108
23. Geisser B, Ponce A, Alsfasser R (1999) pH-dependent excited-state dynamics of $[Ru(bpy)_3]^{2+}$–modified amino acids: effects of an amide linkage and remote functional groups. Inorg Chem 38:2030–2037
24. Mecklenburg SL, McCafferty DG, Schoonover JR, Peek BM, Erickson BW, Meyer TJ (1994) Spectroscopic study of electron transfer in a trifunctional lysine with anthraquinone as the electron acceptor. Inorg Chem 33:2974–2983
25. Striplin DR, Reece SY, McCafferty DG, Wall CG, Friesen DA, Erickson BW, Meyer TJ (2004) Solvent dependence of intramolecular electron transfer in a helical oligoproline assembly. J Am Chem Soc 126:5282–5291
26. Imperiali B, Fisher SL (1992) Stereoselective synthesis and peptide incorporation of (S)-.alpha.-amino-(2,2′-bipyridine)-6-propanoic acid. J Org Chem 57:757–759
27. Imperiali B, Fisher SL (1991) (S)-.alpha.-Amino-(2,2′-bipyridine)-6-propanoic acid: a versatile amino acid for de novo metalloprotein design. J Am Chem Soc 113:8527–8528
28. Alsfasser R, van Eldik R (1996) Novel building blocks for biomimetic assemblies. synthesis, characterization, and spectroscopic and electrochemical properties of new bidentate ligands derived from lysine and cysteine and their complexes with bis(2,2′-bipyridine)ruthenium(II). Inorg Chem 35:628–636
29. Khan SI, Beilstein AE, Smith GD, Sykora M, Grinstaff MW (1999) Synthesis and excited-state properties of a novel ruthenium nucleoside: $5\text{-}[Ru(bpy)_2(4\text{-}m\text{-}4′\text{-}pa\text{-}bpy)]^{2+}$-2′-deoxyuridine. Inorg Chem 38:2411–2415
30. Saito K, Rutherford AW, Ishikita H (2013) Mechanism of proton-coupled quinone reduction in Photosystem II. Proc Natl Acad Sci 110:954–959
31. Kasson TD, Barry B (2012) Reactive oxygen and oxidative stress: N-formyl kynurenine in photosystem II and non-photosynthetic proteins. Photosynth Res 114:97–110
32. Umena Y, Kawakami K, Shen JR, Kamiya N (2011) Crystal structure of oxygenevolving photosystem II at a resolution of 1.9 Å. Nature 473:55–60
33. Mulkidjanian AY, Kozlova MA, Cherepanov DA (2005) Ubiquinone reduction in the photosynthetic reaction centre of Rhodobacter sphaeroides: interplay between electron transfer, proton binding and flips of the quinone ring. Biochem Soc Trans 33:845–850
34. Lenaz G (1998) Quinone specificity of complex I. Biochim Biophys Acta 1364:207–221
35. Dűrr H, Bossmann S (2001) Ruthenium polypyridine complexes. On the route to biomimetic assemblies as models for the photosynthetic reaction center. Acc Chem Res 34:905–917
36. Sommer MG, Schweinfurth D, Weisser F, Hohloch S, Sarkar B (2013) Substituent-induced reactivity in quinonoid-bridged dinuclear

complexes: comparison between the ruthenium and osmium systems. Organometallics 32:2069–2078
37. Okamoto K, Fukuzumi S (2005) Hydrogen bonds not only provide a structural scaffold to assemble donor and acceptor moieties of zinc porphyrin−quinone dyads but also control the photoinduced electron transfer to afford the long-lived charge-separated states. J Phys Chem B 109:7713–7723
38. Magnuson A, Berglund H, Korall P, Hammarström L, Åkermark B, Styring S, Sun L (1997) Mimicking electron transfer reactions in photosystem ii: synthesis and photochemical characterization of a ruthenium(II) tris(bipyridyl) complex with a covalently linked tyrosine. J Am Chem Soc 119:10720–10725
39. Sun L, Hammarström L, Åkermark B, Styring S (2001) Towards artificial photosynthesis: ruthenium–manganese chemistry for energy production. Chem Soc Rev 30:36–49
40. Lü J-M, Rosokha SV, Neretin IS, Kochi JK (2006) Quinones as electron acceptors. X-Ray structures, spectral (EPR, UV–vis) characteristics and electron-transfer reactivities of their reduced anion radicals as separated vs contact ion pairs. J Am Chem Soc 128: 16708–16719
41. Lo KK-W, Lee TK-M (2004) Luminescent ruthenium(II) polypyridine biotin complexes: synthesis, characterization, photophysical and electrochemical properties, and avidin-binding studies. Inorg Chem 43:5275–5282
42. Hamada T, Tanaka S-i, Koga H, Sakai Y, Sakaki S (2003) Kinetic study of the photo-induced electron transfer reaction between ruthenium(ii) complexes of 2,2[prime or minute]-bipyridine derivatives and methyl viologen. Effects of bulky substituents introduced onto 2,2[prime or minute]-bipyridine. Dalton Trans 4:692–698
43. Mellace MG, Fagalde F, Katz NE, Hester HR, Schmehl R (2006) Photophysical properties of the photosensitizer $[Ru(bpy)_2(5\text{-}CNphen)]^{2+}$ and intramolecular quenching by complexation of Cu(II). J Photochem Photobiol A Chem 181:28–32
44. McCusker JK (2003) Femtosecond absorption spectroscopy of transition metal charge-transfer complexes. Acc Chem Res 36:876–887
45. Yeh AT, Shank CV, McCusker JK (2000) Ultrafast electron localization dynamics following photo-induced charge transfer. Science 289: 935–938
46. Görner H (2007) Electron transfer from aromatic amino acids to triplet quinones. J Photochem Photobiol B Biol 88:83–89
47. Gorner H (2004) Photoreactions of p-benzo-, p-naphtho- and p-anthraquinones with ascorbic acid. Photochem Photobiol Sci 3: 933–938
48. Giacco TD, Elisei F, Lanzalunga O (2000) Photoinduced hydrogen- and electron-transfer processes between chloranil and aryl alkyl sulfides in organic solvents. Steady-state and time-resolved studies. Phys Chem Chem Phys 2:1701–1708
49. Esaka Y, Okumura N, Uno B, Goto M (2001) Non-aqueous capillary electrophoresis of quinone anion radicals. Anal Sci 17:99–102
50. Pochon A, Vaughan PP, Gan D, Vath P, Blough NV, Falvey DE (2002) Photochemical oxidation of water by 2-Methyl-1,4-benzoquinone: evidence against the formation of free hydroxyl radical. J Phys Chem A 106:2889–2894
51. Barbara PF, Meyer TJ, Ratner MA (1996) Contemporary issues in electron transfer research. J Phys Chem 100:13148–13168
52. Marcus RA, Sutin N (1985) Electron transfers in chemistry and biology. Biochim Biophys Acta 811:265–322
53. Rehm D, Weller A (1970) Kinetics of fluorescence quenching by electron and H-atom transfer. Israel J Chem 8:259–271
54. Rehm D, Weller A (1969) Kinetik und Mechanismus der Elektronübertragung bei der Fluoreszenzlöschung in Acetonitril. Ber Bunsen Gen Chem 73:834–839
55. Kavarnos GJ, Turro NJ (1986) Photosensitization by reversible electron transfer: theories, experimental evidence, and examples. Chem Rev 86:401–449
56. Smolunchouski MZ (1917) Versuch einer mathematischen theorie der Koagulationskinetik Kolloider Losungen. Phys Chem 92:129–168
57. Fuoss RM (1958) Ionic association. III. The equilibrium between ion pairs and free ions. J Am Chem Soc 80:5059–5061
58. Cang L, Sun H, Hoffman MZ (1997) Ground- and excited-state interactions between the tris(2,2′-bipyridine)ruthenium(2+) ion and phenol in aqueous solution. J Photochem Photobiol A Chem 108: 129–133
59. Borgström M, Johansson O, Lomoth R, Baudin HB, Wallin S, Sun L, Åkermark B, Hammarström L (2003) Electron donor–acceptor dyads and triads based on tris(bipyridine)ruthenium(II) and benzoquinone: synthesis, characterization, and photoinduced electron transfer reactions. Inorg Chem 42:5173–5184
60. Benniston AC, Chapman GM, Harriman A, Rostron SA (2005) Reversible luminescence switching in a ruthenium(II) bis(2,2′:6′,2″-terpyridine)-benzoquinone dyad. Inorg Chem 44:4029–4036
61. Roura-Pérez G, Quiróz B, Aguilar-Martínez M, Frontana C, Solano A, González I, Bautista-Martínez JA, Jiménez-Barbero J, Cuevas G (2007) Remote position substituents as modulators of conformational and reactive properties of quinones. Relevance of the π/π intramolecular interaction. J Org Chem 72:1883–1894